

# Studies on synthesis, bulk growth, optical and mechanical properties of an organic single crystal: L-histidinium maleate for optoelectronic applications

H. ARUL, R. EZHIL VIZHI, D. RAJAN BABU\*

*Crystal Growth and Crystallography Division, School of Advanced Sciences, VIT University, Vellore-632014, India*

L-Histidinium Maleate was synthesized and subsequently good quality single crystals were grown from aqueous solution by slow cooling technique. The grown crystals were subjected to powder X-ray diffraction to confirm the crystallinity. FT-Raman spectra revealed the presence of various functional groups.  $^{13}\text{C}$  NMR analysis confirmed the formation of structure in the title compound. The optical properties of the grown crystals were analyzed by UV-Vis-NIR spectrum. The optical reflectance and extinction coefficient were also calculated for this crystal. The refractive index of the crystal was determined by prism coupling technique. Photoluminescence studies revealed that the material emitted violet emission. Vicker's microhardness studies were carried out to study the mechanical property of the grown crystal. The second harmonic generation of the material was investigated by Kurtz-Perry technique, and the efficiency was estimated to be higher than that of KDP.

(Received April 1, 2014; accepted March 19, 2015)

*Keywords:* Organic crystal, Energy gap, Emission spectra, Vickers Microhardness, SHG

## 1. Introduction

Nonlinear optical materials play an extensive role in the modern optical communication technologies, including frequency shifting, optical switching, optical modulation and optical data storage. Many researchers have engaged in the quest of novel NLO materials. The efficiency in converting infrared radiation to ultraviolet has been a major technological problem, which has attracted much attention in recent times. Explorations towards the novel organic material are especially interesting because they can offer a highly aligned and stable orientation of NLO chromophores in the crystal lattice [1]. Organic materials have gained a great deal of attention due to their inherent ultrafast response times and high optical threshold when compared to the inorganic materials [2]. The engineering and design of organic crystals with intrinsic tailorability, less deliquescence, molecular flexibility have prompted the researchers to probe into the realm of frontier research with NLO Material [3]. The molecular nonlinearity observed with the delocalized  $\pi$  – electrons connected with the donor-acceptor groups belonging to the organic ligand results in the high nonlinear electro optic coefficient [4]. Amino acid crystals have been extensively studied for their superior characteristics by many researchers. Amino acid contains both the donor carboxylic (COOH) and the proton acceptor amino ( $\text{NH}_2$ ) group, known as zwitterions, which create hydrogen bonds. Due to its dipolar nature, it is perfect for optoelectronics applications [5]. Amino acids contain chiral carbon atoms, directing the crystallization in non-centrosymmetric space group and it also possesses zwitterionic nature, which favours crystal hardness [6]. L-Histidine derivatives have attracted attention as promising NLO material after they were found to possess

high NLO properties when compared to other amino acids [7]. In order to improve the nonlinear characteristics of L-Histidine, and to grow good quality crystals, the complexes of amino acids with dicarboxylic acids have already been tried [8,9]. Maleic acid complexes of amino acids have been reported earlier for their efficient nonlinear optical properties [9]. The crystal structure and the nonlinear optical properties of L-Histidinium Maleate have also been reported in the recent past [10, 11].

In the current investigation, we computed optical band gap, optical reflectance, extinction coefficient from the UV-Vis-NIR transmittance data. Functional groups were identified by FT-Raman spectrum. NMR analysis confirmed the structure of the title compound. Refractive index measurement was carried out for the first time by prism coupling technique. Photoluminescence studies revealed the emission spectra of the sample. Vicker's hardness number ( $H_v$ ), work hardening coefficient ( $n$ ) and elastic stiffness constant were also calculated. All the results are discussed in detail.

## 2. Experimental

### 2.1 Synthesis and Crystal Growth

The title compound was synthesized with the AR Grade of L-Histidine and Maleic acid in an equimolar ratio, and the calculated amount of material was dissolved in Millipore water at room temperature. The solubility of the LHM salt was determined gravimetrically in the range of  $30^\circ\text{C}$  to  $50^\circ\text{C}$ . The material had positive temperature coefficient of solubility which alleviated the growth by slow cooling as seen in figure.1. The slow cooling method

was adopted to grow bulk LHM crystal using constant temperature bath with an accuracy of  $\pm 0.01^\circ\text{C}$ . The synthesized and recrystallized LHM salt was used to prepare the saturated solution. The saturated solution of LHM was prepared at  $45^\circ\text{C}$  based on solubility data, and the saturation was achieved by maintaining the growth solution at  $45^\circ\text{C}$  in constant temperature water bath for 2 days. The solution was initially cooled at a rate of  $0.01^\circ\text{C}/\text{day}$ , and subsequently  $0.02^\circ\text{C}/\text{day}$  followed by  $0.1^\circ\text{C}/\text{day}$ , as the growth progressed. Under optimum conditions, high quality crystals of typical dimensions of  $23 \times 19 \times 4 \text{ mm}^3$  (Fig.2) were grown in about 19 days.

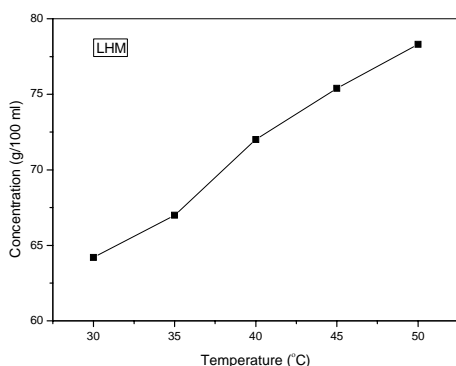


Fig.1 Solubility curve of LHM

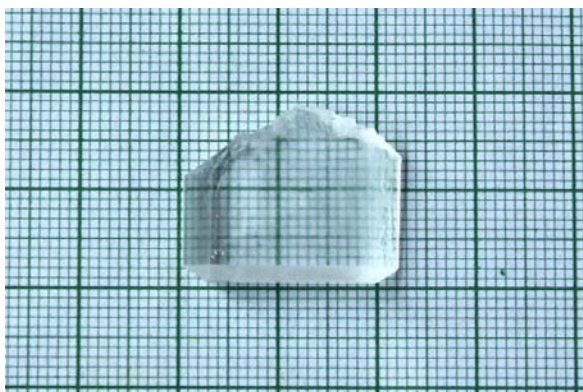


Fig.2 As grown crystal of LHM

### 3. Results and Discussions

#### 3.1 Powder X-ray diffraction

The purity and crystalline nature of LHM crystals were confirmed by recording powder X-ray diffraction pattern using Bruker D8 Advance, employing  $\text{Cu K}\alpha$  ( $1.5048 \text{ \AA}$ ) with a scan speed of  $2^\circ/\text{min}$  over a range of  $10\text{--}80^\circ$ .

The diffraction pattern is shown in Fig. 3. The obtained peaks were indexed using Powder X. The calculated cell parameters were  $a = 11.4735 \text{ \AA}$ ,  $b = 8.0621 \text{ \AA}$ ,  $c = 14.982 \text{ \AA}$  and  $\alpha = \gamma = 90^\circ$ ,  $\beta = 101.691^\circ$ . The title compound crystallized in the monoclinic system with  $P2_1$  space group. These values are in good agreement with the reported values [11].

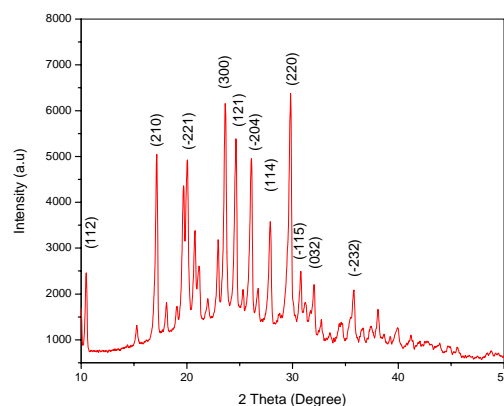


Fig.3 Powder XRD Pattern of LHM Crystal

#### 3.2 Spectral Studies

##### 3.2.1 FT-RAMAN Analysis

FT-Raman analysis was carried out to understand the presence of various functional groups using Bruker RFS-27 stand alone FT-Raman spectrometer in the range of  $3000\text{--}500 \text{ cm}^{-1}$ . The FT-Raman spectrum is shown in Fig. 4. The different assignments which support the investigation are tabulated (Table. 1)

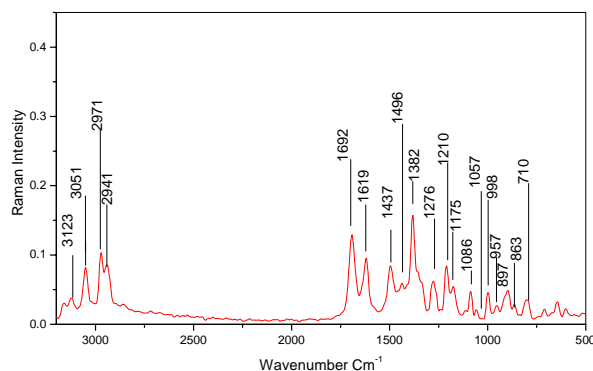


Fig.4 FT-Raman Spectrum of L-Histidinium Maleate

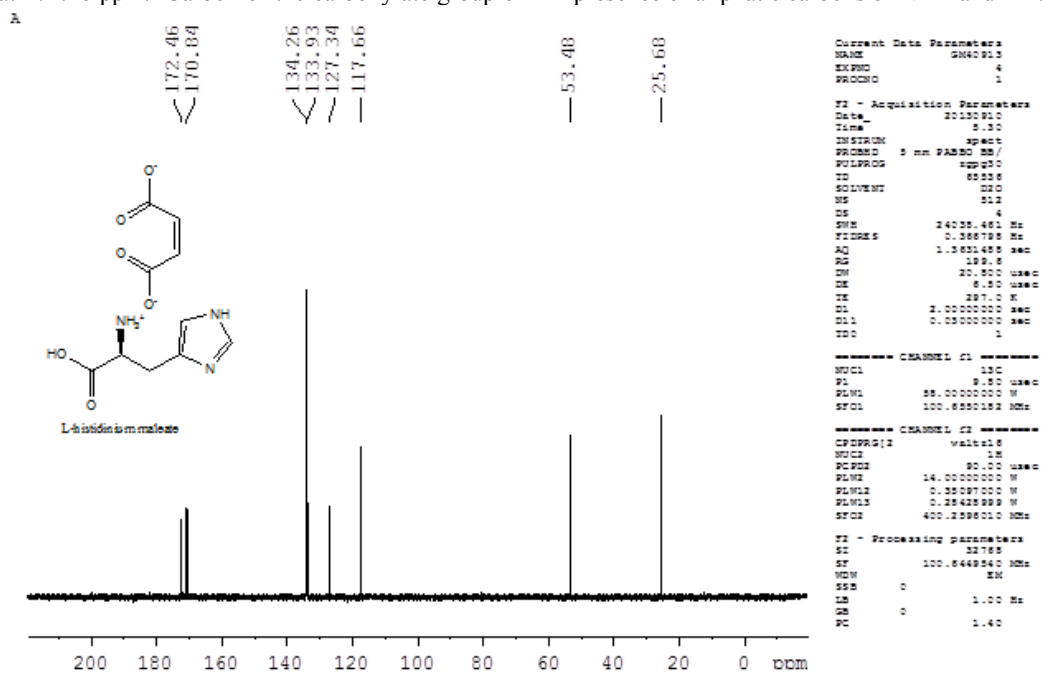
Table.1. FT-Raman Spectrum of L-Histidinium Maleate

S. No	Observed	Assignment
1	3123	Aromatic C-H Stretch
2	3051	Aliphatic C-H Stretch of Maleate
3	2971	CH (CH <sub>2</sub> ) Stretching
4	2941	Symmetric Stretching of NH
5	1692	Symmetric Stretching of C=O in COOH
6	1619	Asymmetric Stretching of C=C in Maleate
7	1496	Symmetric bending of NH <sup>3+</sup>
8	1437	Bending of CH <sub>2</sub>
9	1382	Symmetric stretching of COO <sup>-</sup>
10	1276	Symmetric stretching of C-H
11	1210	Bending of C-OH
12	1175	Out of plane bending of CH <sub>2</sub>
13	1086	In plane bending of NH <sup>3+</sup>
14	1057	C-N Stretching
15	998	Out of plane bending of C-H
16	897	C=CH <sub>2</sub> Stretching
17	863	C-C-O Stretch
18	710	COO <sup>-</sup> deformation
19	644	C-H bending

### 3.2.2 <sup>13</sup>C NMR Spectral Analysis

<sup>13</sup>C NMR spectrum was used to identify the carbon atom present in various chemical environments, and to confirm the functional groups in the grown LHM Crystal. Figure.5 shows the recorded <sup>13</sup>C NMR Spectrum. Carbon atom in carboxyl group of L-histidinium is shown by the signal at 172.46 ppm. Carbon of the carboxylate group of

Maleate ion was observed at 170.84 ppm. Signal at 134.26 ppm confirmed the ortho carbon of the alkyl substituent. Equivalent carbon of the Maleate ion was observed at 133.93 ppm and ring carbon of the alkyl substituent was seen at 127.34 ppm. The signal at 117.66 ppm showed the presence of Meta carbon of the alkyl substituent. The signals at 53.48 ppm and 25.68 ppm confirmed the presence of aliphatic carbons of NH<sup>3+</sup> and Imidazole ring.

Fig. 5. <sup>13</sup>C NMR Spectrum of L-Histidinium Maleate

### 3.3 Optical Studies

#### 3.3.1 UV-Vis-NIR Spectral Studies

The main requirements for optoelectronics device applications are optical transmittance range and cut-off wavelength [12]. UV-Visible spectral analysis is an efficient tool to determine the optical transparency of the crystals. This is an important property for a material to be optically active [13]. UV-Vis-NIR optical transmission spectrum was recorded in the range of 190-900 nm for LHM crystal of thickness 2 mm at room temperature using U-2800 spectrophotometer. The transmittance spectra of LHM sample (Fig. 6) showed large absorption at 370nm. This was due to  $n-\pi$  transition of the carbonyl group of carboxyl function [14]. The dependence of optical absorption coefficient with the photon energy helped us study the band structure and type of transition of electrons [15].

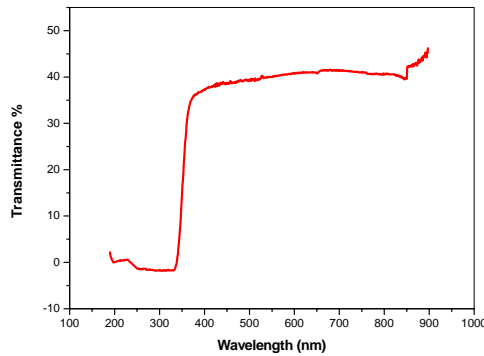


Fig. 6. UV-Vis-NIR transmission spectra of LHM crystal

#### 3.3.2 Optical band gap energy ( $E_g$ )

The crystal should have high transparency in the considerable region of wavelength for optical device fabrication [16, 17]. The cut-off wavelength for LHM crystal was found to be at 370 nm, thus making it a potential material for optical device fabrication. The optical absorption coefficient ( $\alpha$ ) was calculated using the relation

$$\alpha = 2.3026 (1/T)/t \quad (1)$$

Where T is the transmittance and t is the thickness of the crystal.

The energy dependence of absorption coefficient of the crystal for high photon energies ( $h\nu$ ) is given by the following equation [18],

$$h\nu = A \sqrt{h\nu - E_g} \quad (2)$$

Where A is the constant,  $E_g$  the optical band gap, h the Planck's constant and  $\nu$  the frequency of incident photons.

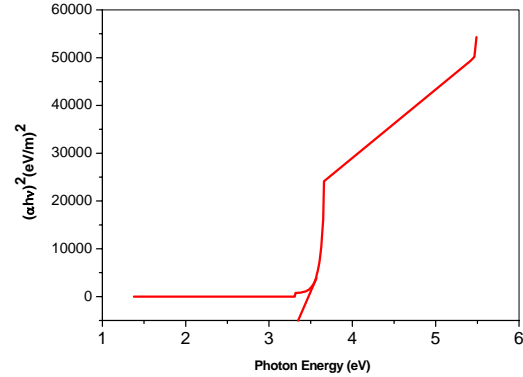


Fig. 7. Photon energy vs.  $(ah\nu)^2$  for LHM crystal

A graph was plotted between  $(h\nu)$  and  $(ah\nu)^2$  using Tauc's relation to estimate the direct band gap value (Fig. 7), where  $\alpha$  was the absorption coefficient and  $h\nu$  was the energy of the incident photon [19]. The energy gap was determined by extrapolating the linear portion of the curve near the onset of absorption to  $(h\nu\alpha)^2 = 0$  [20]. From the plot, the band gap of LHM crystal was found to be 3.31 eV.

The optical constants ( $n, k$ ) were determined from the transmittance (T) and reflectance (R) spectrum based on the following relations [20]

$$T = (1 - R)^2 \exp(-\alpha t) / (1 - R^2 \exp(-2\alpha t)) \quad (3)$$

Where t is the thickness and  $\alpha$  is related to extinction coefficient

$$k = \alpha \lambda / 4\pi \quad (4)$$

The refractive index can be determined from the reflectance (R) data using the relation [18]

$$R = (n - 1)^2 / (n + 1)^2 \quad (5)$$

The reflectance in terms of absorption coefficient can be written as

$$R = 1 \pm \sqrt{1 - \exp(-\alpha t) + \exp(\alpha t) / (1 + \exp(-\alpha t))} \quad (6)$$

And from the above equation, the refractive index n can also be derived as

$$n = -(R + 1) \pm \sqrt{3R^2 + 10R - 3} / 2(R - 1) \quad (7)$$

Fig. 8 shows the variation extinction coefficient as a function of photon energy. Since the internal energy of the device also depends on photon energy, one can achieve the desired material to fabricate the optoelectronic devices by tailoring the photon energy and absorption coefficient [20]

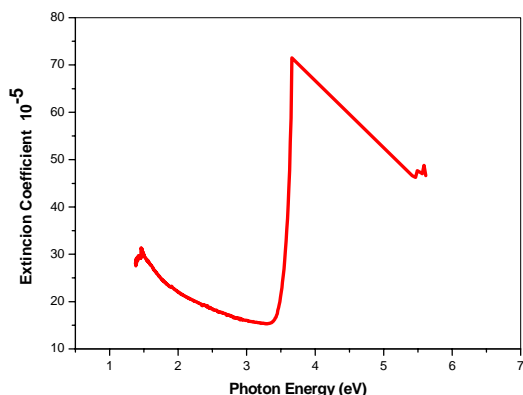


Fig. 8. Plot of Photon energy vs. Extinction coefficient

### 3.4 Refractive index analysis

The Refractive index coefficients are more important parameters in the design of solid state laser. Sensitive determination of the refractive indices of certain materials is very important in materials research [21]. The Refractive index of L-Histidinium Maleate was measured using a Metricon prism coupler model 2010/M in TE mode. The resolution of the instrument was  $\pm 0.0003$ . A laser beam was allowed to strike the base of the prism, and was normally reflected at the prism base onto a photodetector. The crystal to be measured was brought in contact with the prism by means of pneumatically operated coupling head, such that an air gap separated the sample and the prism. The angle of incidence ' $\theta$ ' of the laser beam was varied by means of rotary table upon which the prism, crystal, coupling head, and photodetector were mounted. At certain values of  $\theta$ , called mode angle, photons violated the total internal reflection criterion, and tunnelled from the base of the prism across the air gap and into the crystal and entered optical propagation modes, causing a sharp drop in the intensity of light striking the photodetector. The knee was located at the table position of -993 and at the angle of incidence was observed at  $-12.9^\circ$ . The index was calculated by an appropriate computer algorithm. Figure.9 shows the mode profile which was determined by measuring the reflected intensity vs. the angle of incidence (in degrees). For device fabrication such as waveguide, the property of index profile is required. Hence, the index measurement of the mirror polished crystal was measured using He-Ne laser with a wavelength of 632.8 nm, and the refractive index was found to be 1.4919. The refractive index analysis provides the possibility of studying the optical waveguide nature of the grown crystal.

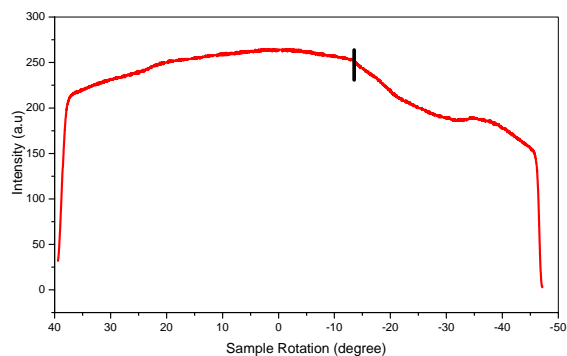


Fig. 9. Reflected intensity vs. angle of incidence (in degrees).

### 3.5 Photoluminescence Studies

Photoluminescence (PL) measurement is a prominent tool for determining the crystalline quality of a system as well as identifying its exciton fine structure [22]. The PL analysis of L-histidinium Maleate was carried out using Jobin Yvon-Spex spectrofluorometer with 450W high pressure xenon lamp as an excitation source. The emission spectrum (Fig.10) was recorded in the wavelength region from 300 to 700 nm. The excitation wavelength for the sample was chosen as 285 nm. A strong emission was observed at 389 nm. The emission spectrum gave the evidence that LHM Crystal was efficient for absorption of ultraviolet light and the emission of light in the violet region.

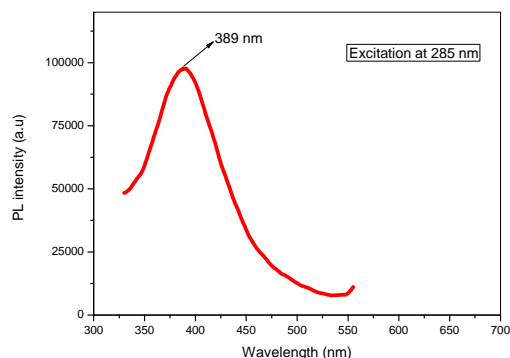


Fig. 10. Photoluminescence Spectrum

### 3.6 Microhardness Studies

We studied the mechanical property of the grown crystal at room temperature using MATSUZAWA model MMT-X series fitted with a Vicker's diamond pyramidal indenter with a dwell time of 5 s. The diagonal length of indentation impression was carried out using a microscope. The indentation marks were made on the surface by varying the load from 5 g to 100 g. The microhardness value was calculated using the formula:

$$H_v = 1.8544 P / d^2 \text{ kg/mm}^2 \quad (8)$$

Where  $H_v$  is the hardness number,  $P$  is the applied load;  $d$  is the diagonal length of the indentation. Fig. 11 shows the variation of hardness number ( $H_v$ ) as a function of applied load ranging from 5 g to 100 g. The hardness number increased with increasing load. This is termed as Reverse Indentation Size Effect (RISE).

This might be due to the nucleation and motion of dislocations and point defects produced by indentation on the crystal surface [23].

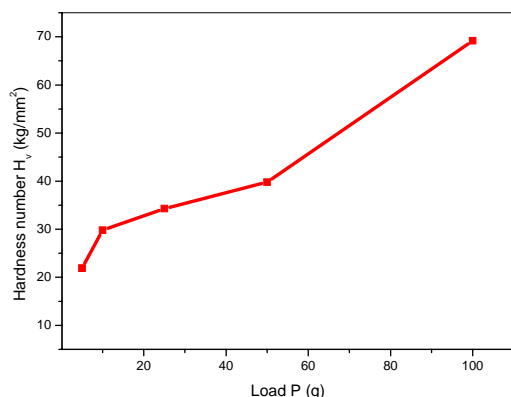


Fig. 11. Load  $P$  (g) vs. Hardness number ( $H_v$ )

The work hardening coefficient ( $n$ ) is the strength of the crystal. The value of  $n$  lies between 1 and 1.6 for hard materials and it is greater than 1.6 for softer materials [24]. A graph was plotted between  $\log P$  Vs.  $\log d$  as shown in Figure.12. The slope of the line gave the value of ' $n$ '. The work hardening coefficient ( $n$ ) for LHM was found to be 2.36, which showed that LHM belonged to the soft material category.

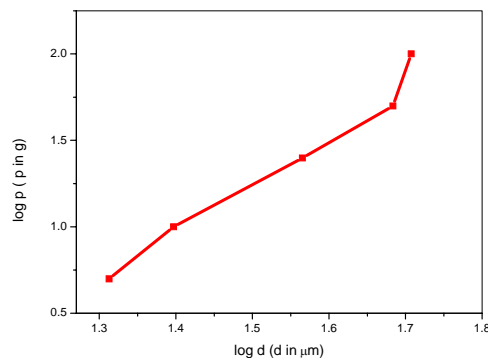


Fig. 12. Plot of  $\log d$  vs  $\log p$

The elastic stiffness constant ( $C_{11}$ ) gives the measure of resistance to deformation by a applied load on the flat crystal surface. The value of ( $C_{11}$ ) is determined by two important factors - tightness of bonding between the neighbouring atoms and the rate of variation with positions of the atoms of the forces of attraction and repulsion between them [25]. The elastic stiffness constant ( $C_{11}$ ) was calculated by Wooster's empirical relation  $C_{11} = (H_v)^{7/4}$  [26]. The calculated stiffness constant for different loads is tabulated in Table 2. The difference in the elastic stiffness constant of LHM crystals was due to the bond strength between the ions in the crystalline materials [27].

Table. 2 Elastic stiffness constant of LHM

Load (g)	$H_v$ (kg/mm <sup>2</sup> )	$C_{11} \times 10^{14}$ (Pa)
5	21.9	0.68
10	29.8	1.17
25	34.3	1.50
50	39.8	1.95

### 3.7 SHG test

The SHG efficiency of LHM crystal was measured by the Kurtz and Perry powder technique [28]. A Q-Switch mode locked Nd:YAG Laser with first harmonic output at 1064 nm, with an input power of 3.3mJ. SHG behaviour was confirmed by the emission of green light from the powdered sample of LHM with an output of 18.6 mV. Powdered KDP sample was used as a reference material in the measurement with the output of 7 mV. It showed that the SHG efficiency of LHM Sample was 2.6 times greater than KDP.

#### 4. Conclusion

Good quality optical single crystal of L-Histidinium Maleate was grown by slow cooling technique. The unit cell parameters and crystalline perfection of grown crystals were confirmed by Powder X-ray diffraction. Functional groups were identified using FT-Raman spectrum. The structure of the LHM was confirmed by  $^{13}\text{C}$ NMR spectroscopy. The optical behaviour was evaluated by UV-Vis-NIR spectrum. Refractive index of the crystal was found to be 1.4919, using prism coupling technique. Photoluminescence spectrum revealed the violet emission of the material at 389nm. This confirmed the suitability for opto-electronic applications. The Vickers microhardness study of the LHM crystal revealed that the hardness number  $H_v$  increased with the increasing load. The value of work hardening coefficient was found to be greater than 1.6 for LHM. The grown crystal falls under the soft material category. The existence of SHG was confirmed by the Kurtz-Perry powder test

#### Acknowledgement

The authors thank DST-SERB, Government of India for funding this research project (SR/S2/CMP-02/2011). The authors are grateful to the management, VIT University, Vellore for providing the excellent research facilities. The authors express their thanks to Dr.R. Mohankumar, Presidency College, Chennai for providing the UV-Vis-NIR spectroscopy. The authors would like to thank Dr. R. Gopalakrishnan, Anna University, Chennai for providing the Vickers microhardness tester

#### References

- [1] M. Thakur, J.Xu, A. Bhowmik, L.Zhou: Appl. Phys Lett, **74**, 635 (1999)
- [2] T. Pal, T. Kar, G. Bocelli, L. Rigi: Cryst Growth Des. **3**, 13 (2003)
- [3] A. Gavezzotti: Curr. Opin. Solid State Mater. Sci. **1**, 501 (1996)
- [4] H.S. Nalwa: Adv. Mater. **5**, 341 (1993)
- [5] B.A. Fuchus, C.K. Syn, S.P. Velsko: Appl.opt. **28**, 4465 (1989)
- [6] P. Kumaresan, S. Moorthy Babu, P.M. Anbarasan: Opt. Mater. **30**, 1361 (2008)
- [7] H. O. Marcy, M. J. Rosker, L. F. Warren, P. H. Cunningham, C.A. Thomas, L. A. DeLoach, S. P. Velsko, C. A. Ebbers, J. H. Liao, M. G. Kanatzidis: Opt. Lett, **20**, 252 (1995)
- [8] C. Ramachandraraja, A. Anthony Joseph: Mater. Lett. **64**, 108 (2010)
- [9] S. Natarajan, S.A. Martin Britto, E. Ramachandran: Cryst. Growth Des. **6**, 137 (2006)
- [10] M. Fleck, V.V. Ghazaryan, L.S. Bezhanova, A.K. Atanesyan, A.M. Petrosyan: J. Mol. Struct. **1035**, 407 (2013)
- [11] C.A. Gonsago, H.M. Albert, J. Karthikeyan, P. Sagayaraj, A.J. Arul Pragasam: Mater. Res. Bull. **47**, 1648 (2012)
- [12] R.M.Silverstein, F.X. Webster, David Kiemle: Spectrometric identification of Organic Compounds (John Wiley Eastern & Sons Inc. Canada 1998)
- [13] C.N.R. Rao: Ultraviolet and Visible Spectroscopy (Butterworths, London 1975)
- [14] D. Comoretto, L. Rossi, A. Borghesi: J. Mater. Res. **12**, 1262 (1997)
- [15] N. Kejalakshmy, K. Srinivasan: Opt. Mater. **27**, 389 (2004)
- [16] V. Krishnakumar, R. Nagalakshmi: Spectrochim. Acta, Part A. **61**, 499 (2005)
- [17] V. Krishnakumar, R. John Xavier: Spectrochim. Acta, Part A. **60**, 709 (2004)
- [18] A. Ashour, N. El-Kadry, S.A. Mahmoud: Thin Solid Films. **269**, 117 (1995)
- [19] J. Tauc, R. Girgorovici, A. Vancu: Phys. Stat. Sol. B. **15**, 627 (1996)
- [20] R.E. Denton, R.D. Campbell, S.G. Tomlin: J. Phys. D: Appl. Phys. **5**, 852 (1972)
- [21] Shyam Singh, Phys. Scr. **65**, 167 (2002)
- [22] L. Kumari, W.Z. Li: Cryst. Res. Technol. **45**, 311 (2010)
- [23] K. Sangwal: Mater. Chem. Phys. **63**, 145 (2000)
- [24] E.M. Onitsch: Mikroskopie. **2**, 131 (1947)
- [25] N. Sudharshana, B. Keerthana, R. Nagalakshmi, V.Krishnakumar, L. Guruprasad: et.al, Mater. Chem. Phys. **134**, 736 (2012)
- [26] W.A. Rooster: Rep. Progr. Phys. **16**, 62 (1953)
- [27] Susmita Karan, S. P. Sen Gupta: Mater.Sci.Eng. A. **398**, 198 (2005)
- [28] S.K.Kurtz, T.T. Perry: J. Appl. Phys. **39**, 3798 (1968)

\*Corresponding author: rajanbabuphy@gmail.com